Available online at www.sciencedirect.com
ScienceDirect
Colloids and Surfaces A: Physicochem. Eng. Aspects 303 (2007) 191–200
COLLOIDS AND SURFACES A
www.elsevier.com/locate/colsurfa

The dielectric spectrum and the electrorheological effect in suspensions of varying conductivity Part 2. Modeling of the electrorheological effect

F. Bautista [a], L. Rejón [b,*], O. Manero [c]

[a] *Departamento de Física, Universidad de Guadalajara, Blvd. M. García Barragán 1451, Guadalajara, Jal. 44430, Mexico*
[b] *Gerencia de Materiales y Procesos Químicos, Instituto de Investigaciones Eléctricas, Calle Reforma 113, Colonia Palmira Cuernavaca, Mor. 62490, Mexico*
[c] *Instituto de Investigaciones en Materiales, Universidad Nacional Autónoma de México, A.P. 70-360, México, D.F., Mexico*

Received 22 June 2006; received in revised form 16 March 2007; accepted 27 March 2007
Available online 12 April 2007

Abstract

In this part, attention is given to the electrorheological effect of suspensions of polarizable particles in three different liquids of varying conductivity. The electrorheological properties of the suspensions are analyzed with a kinetic model that describes the flow-induced modification of the structures formed by the particles under dc electric fields. Under quiescent conditions, the model describes the variation of viscosity of the suspension with the electric field and particle concentration, as well as the change in the yield stress with electric field. The effect of non-linear conductivity is introduced in the model to account for the trend towards saturation observed in the viscosity at high electric fields and particle concentration. Furthermore, the contribution of non-linear conduction in the model allows the prediction of the yield stress at high electric fields. The model further describes the variation of viscosity with shear rate under a given electric field, and time-dependent phenomena arising from the dynamics of the breakage-reformation process of the structures.

Keywords: Electrorheology; Rheological modeling; Conductivity; Suspensions

1. Introduction

According to the dielectric analysis exposed in Part 1 [1], it is known that the interfacial polarization of the particles affects the electric-field induced-aggregation in electrorheological fluids. Likewise, the thermodynamic properties of the suspension are strongly influenced by the dielectric relaxation. The dependence of the thermodynamic driving force which causes the aggregation of particles on the value of the electric field is caused by dielectric relaxation. As mentioned in Part 1, the presence of the dielectric relaxation phenomena leads to the redistribution of the charge at the interface between the particle and the surrounding field. The relaxation time for the charge redistribution (characteristic time scale of the dielectric relaxation) caused by the particle and fluid conductivity is given by

$$t_{\mathrm{P}} = \varepsilon_0 \frac{\varepsilon_{\mathrm{P}} + 2\varepsilon_{\mathrm{f}}}{\sigma_{\mathrm{p}} + 2\sigma_{\mathrm{f}}}, \tag{1}$$

where ε_{p} is the particles permittivity, ε_{f} and ε_0 the fluid and vacuum permittivities, and σ_{p} and σ_{f} are the particles and fluid conductivities [2].

In dc electric fields the particles aggregate only provided that a certain relation between the ratio of the particle-to-suspending liquid dielectric constants and that of the conductance is satisfied. Hence, a correlation exists between the ER activity of a suspension and its dielectric spectrum. Two limit cases can be observed, first, when $t \ll t_{\mathrm{p}}$, there is no contribution of the conductivity effects to the inter-particle interaction, or equivalently, the situation corresponds to non-conducting particles in a non-conducting fluid. Second, when $t \gg t_{\mathrm{p}}$, conductivity effects

* Corresponding author. Tel.: +52 777 3623831; fax: +52 777 3623832.
E-mail address: lrejon@iie.org.mx (L. Rejón).

0927-7757/$ – see front matter © 2007 Elsevier B.V. All rights reserved.
doi:10.1016/j.colsurfa.2007.03.051

Nomenclature

A	measure of structure changes due to the flow and electric fields
D	rate of strain tensors
E	the applied electric field
G_0	the elastic modulus
k_0'	kinetic function (flow)
k_1'	kinetic function (electric)
k_2	constant
Mn	Mason number
Mn^*	material constant
$N(t)$	chain size
$N(t)_{\max}$	maximum stable size of the chains
t_a	characteristic time scale for structure formation
t_p	relaxation time for the charge redistribution (characteristic time scale of the dielectric relaxation)

Greek letters

β	$(\varepsilon_p-\varepsilon_f)/(\varepsilon_p+2\varepsilon_f)$
$\dot{\gamma}$	shear rate
ε_o	permittivity of free space, ε_p, and ε_f are the static dielectric constants of particles and dispersing medium
η	viscosity
η_E	viscosity induced by electric field
η_0	Newtonian viscosity
λ	the structure relaxation time
λ_E	the relaxation time at high electric fields
λ_0	the Maxwell relaxation time
λ_∞	the relaxation time at high deformation rates
σ	conductivity, σ_p, and σ_f are the conductivities of the particles and medium
$\boldsymbol{\tau}$	stress tensor
τ	shear stress
τ_y	yield stress
τ_{y0}	yield stress at zero electric field
$\overset{\nabla}{\tau}$	upper-convected time derivative of the stress tensor

contribute mainly to the inter-particle interaction. Let t_a be the characteristic time scale for structure formation, which may be estimated by considering the time taken for a particle to move a characteristic distance between the particles. In dc electric fields, the inter-particle forces are determined by the interfacial polarization which governs the ratio of the time scale of the particle motion to the time scale of the dielectric relaxation t_a/t_p. When this ratio is much smaller than one for strong dc electric fields, the inter-particle forces are determined only by the ratio of the particle-to-suspending liquid dielectric constants and a threshold value of the electric field always exists, above which the particles having $\varepsilon_p \neq \varepsilon_f$ will start aggregating as soon as the electric field has been applied. When the ratio is larger than one under weak dc electric fields, aggregation will occur if a certain relation between the ratio of the particle-to-suspending liquid dielectric constants and that of the conductance is satisfied.

The electric field induces alignment of suspended particles into chains and columns aggregated parallel to the electric field lines. The external flow in turn modifies the alignment of chains and can lead to fragmentation. For steady shear flow, the balance between the hydrodynamic and electrostatic polarization forces can be described by the Mason number, i.e.,

$$Mn = \frac{\eta\dot{\gamma}}{2\varepsilon_0\varepsilon_f\beta^2 E_0^2}, \tag{2}$$

where $\beta=(\varepsilon_p-\varepsilon_f)/(\varepsilon_p+2\varepsilon_f)$, $\dot{\gamma}$ is the shear rate and η is the viscosity.

The prediction of the electrorheological effect involves a mathematical model which in principle should be capable to account for the formation of structures induced by the electric field and the fragmentation of such structures under flow. The model should contain definite constants (material properties) that one can measure (permittivities, conductivities, first and second Newtonian viscosities, and others) and it should be able to predict the experimental results once the material properties are known.

The description of structural changes due to either electric field or external flow usually involves a kinetic process of structure modification. The balance between electrostatic polarization forces, hydrodynamic forces and thermal forces has been analyzed by the so-called kinetic models. As an example, a kinetic chain model has been proposed by Martin and Odinek [3]. The model is based on the assumption that dipolar interactions and hydrodynamic forces dominate thermal forces (as is certainly clear in non-Brownian suspensions). The model further assumes a maximum stable size of the chains $N(t)_{\max}$, and this dimension results from a balance between aggregation and fragmentation. The kinetics of aggregation and fragmentation follows a phenomenological expression

$$\frac{\mathrm{d}N(t)}{\mathrm{d}t} = \frac{k_M}{N(t)}\left[1-\frac{N(t)^2}{N(t)_{\max}^2}\right] \tag{3}$$

The aggregation process is induced by the dipolar forces and hence the kinetic constant k_M is given by

$$k_M = k_{0M}\left(\frac{8\varepsilon_0\varepsilon_f\beta^2 E_0^2}{\eta_0}\right) \tag{4}$$

where k_{0M} is a concentration-dependent kinetic constant. Eq. (3) has various asymptotic limits: when the chain reaches its maximum length no aggregation or fragmentation occurs since $N(t)$ is constant. When $N(t) \ll N(t)_{\max}$, which means that the chain is much smaller than the maximum size, then $N(t)$ is proportional to $\sqrt{t}$. In this case, the chains aggregate slowly, in agreement with predictions of See and Doi [4]. Finally, when $N(t)_{\max} \ll N(t)$ the chains are larger than their maximum stable length, then the chains will fragment exponentially quickly. The fragmentation rate is thus independent of the electric field.

This model predicts a viscosity proportional to the electric field squared and to inverse shear rate according to:

$$\eta = \frac{3\sqrt{6}}{10}\varepsilon_0\varepsilon_f\beta^2\phi E_0^2\dot{\gamma}^{-1} \quad (5)$$

ϕ is the volume fraction of particles.

Eq. (5) gives the simple shear-thinning behavior of a Bingham fluid, corresponding to the presence of a real yield stress, and which is consistent with experimental data at high fields. At low fields, a shear-thinning exponent of around −2/3 is observed.

One of the aims of the present work is to propose a model that can capture the behavior of electrorheological suspensions under dc electric fields when a specific external flow is applied. The model predictions are compared with experimental data taken in electrorheological suspensions made with non-conductive particles and liquids of different conductivities.

2. Experimental part

The electrorheological fluids employed in this study and the preparation methods are the same as those reported elsewhere [5]. Suspensions of silica particles (Merck 60, 15–40 μm) in silicon oil, dioctyl phthalate and tricresyl phosphate with volume fractions between 0.03 and 0.16 were prepared, using a Cowles-type mixer running at 3000 rpm during 10 min. Data on the permittivity, conductivity and viscosity of the suspensions were disclosed in Part 1 (Table 1). The electrorheological suspensions were placed in a vacuum chamber to extract the air bubbles prior to the rheological measurements.

The rheological properties of the suspension were evaluated in a Carri-med CLS 500 controlled-stress rheometer, adapted with an electro-polarizable cell. The measuring cell includes parallel-plate geometry with 4 cm diameter. Electrode separation gap was fixed at 0.75 mm and the voltage (dc) was supplied by a Bertan high-voltage power source (Model 205 B-10R). The applied electric fields ranged from 0.5 to 2 kV/mm at 30 °C.

3. The model

The model proposed in this work examines suspensions of rigid particles dispersed in a liquid continuous phase, by postulating a generally valid invariant constitutive equation. The system under study exhibits time-dependent, reversible, and isothermal decrease of viscosity with shear flow. Conversely, the suspension viscosity will increase upon application of an external electric field. The equilibrium steady-state viscosity represents a dynamic balance between the processes of buildup and breakdown of structure. We therefore assume that the rate of spontaneous buildup of structure, represented by increasing viscosity, depends on the rate at which electric work is done on the suspension and on the Brownian motion. The rate of breakdown of structure (or decreasing viscosity), on the other hand, will depend on the rate at which shear work is done on the suspension [6]. Moreover, electrorheological suspensions possess elasticity and exhibit viscoelastic phenomena. This suggests that the constitutive equation of the material can be an invariant nonlinear model, such as an Oldroyd-type equation of state, i.e., the convected Maxwell equation, but with a time-dependent relaxation time. The relaxation time may be proportional to a scalar which itself follows a kinetic equation representing the balance between the two referred processes. The first process is a spontaneous buildup of structure, which always occurs as the electric field polarizes the particles and they become arranged in specific structures. The second process is the breakdown of the structure induced by the flow strength. The last ingredient of the model assumes that the breakdown of structure depends on the rate at which shear work and electric work are done on the material.

The model proposed here is given by the following set of equations:

$$\underline{\underline{\tau}} + \lambda'(\underline{\underline{\tau}}, \underline{\underline{D}})\overset{\nabla}{\underline{\underline{\tau}}} = 2G_0\lambda'(\underline{\underline{\tau}}, \underline{\underline{D}})\underline{\underline{D}} \quad (6)$$

$$\lambda'(\underline{\underline{\tau}}, \underline{\underline{D}}) = A^{-1}\lambda_0 \quad (7)$$

$$\frac{dA}{dt} = \frac{1}{\lambda}(1-A) + k_0'\left(\frac{\lambda_0}{\lambda_\infty} - A\right)W_F + k_1'\left(\frac{\lambda_0}{\lambda_E} - A\right)W_E \quad (8)$$

τ and D are the stress and rate of deformation tensors, respectively, $\overset{\nabla}{\tau}$ denotes the upper-convected time derivative of the stress tensor, G_0 is the elastic modulus at high frequencies and A is a scalar, representing the suspension structure as function of the flow and electric fields. The four characteristic times are λ, the structure relaxation time, λ_0, the Maxwell relaxation time, λ_∞, the relaxation time at high deformation rates, and λ_E, the relaxation time at high electric fields. k_0' and k_1' are kinetic functions. The expressions for the flow and electric works can be given by:

$$W_F \propto \underline{\underline{\tau}} : \underline{\underline{D}} \quad (9)$$

$$W_E = \underline{E} \cdot \underline{P} \propto \varepsilon_0\varepsilon\beta^2|\bar{E}|^2, \quad (10)$$

where E and P are the electric field and polarization vectors, respectively, $|\bar{E}|$ the magnitude of the applied electric field and

Table 1
Characteristic of solid and liquid phases

Materials	Permittivity, 60 Hz	Conductivity (S cm^{-1})	Viscosity (mPa s)
Silica (Merck 60, 0.015–0.040 mm)	10.9	2.0×10^{-9}	–
Silicon oil (S100)	2.40	6.8×10^{-16}	95
Dioctyl phatalate (DOP)	4.60	2.3×10^{-11}	50
Tricresyl phosphate (TCP)	6.10	1.4×10^{-9}	50

ε is the suspension permittivity, given by a simple mixing rule:

$$\varepsilon = \phi\varepsilon_{\mathrm{p}} + (1-\phi)\varepsilon_{\mathrm{f}}. \tag{11}$$

In the following, $|\bar{E}|$ will be simply denoted by E.

To complete the model description, the kinetic functions are given by the following expressions in terms of the electric field parameters, i.e.,

$$k_0' = \frac{k_0}{1 + k_2\varepsilon_0\varepsilon\beta^2\phi E^2} \tag{12}$$

$$k_1' = k_1\phi \tag{13}$$

In terms of the viscosity of the system, and following the expression of the Maxwell model,

$$\lambda' = \frac{\eta}{G_0} \tag{14}$$

Substitution of Eqs. (9)–(14) into Eq. (8), the kinetic equation becomes:

$$\frac{\mathrm{d}A}{\mathrm{d}t} = \frac{(1-A)}{\lambda} + \frac{k_0(\lambda_0/\lambda_\infty - A)\underline{\underline{\tau}} : \underline{\underline{D}}}{1 + k_2\varepsilon_0\varepsilon\beta^2\phi E^2} + k_1\left(\frac{\lambda_0}{\lambda_{\mathrm{E}}} - A\right)\varepsilon_0\varepsilon\beta^2\phi E^2 \tag{15}$$

The second term on the right-hand side depends on the expression assigned to k_0' Eq. (12). This expression is justified as it represents a balance between the work per unit time (or dissipated energy per unit time) due to the flow and the work per unit time of the electric field. When E vanishes and the flow strength predominates, the second term can be much larger than the third term. Conversely, when E is large, the third term can be much larger than the second one, depending on the magnitude of the viscous dissipation represented by the numerator of the second term.

Specific particular cases may be derived from Eqs. (6)–(8). For example, when elastic effects are small, a "Newtonian" approximation can be obtained, namely:

$$\tau = \frac{\eta_0}{A}\dot{\gamma} \tag{16}$$

$$\frac{\mathrm{d}A}{\mathrm{d}t} = -Aa + \frac{1}{A}b + c, \tag{17}$$

where

$$a = \lambda^{-1} + k_1\varepsilon_0\varepsilon\beta^2\phi E^2, \quad b = \frac{k_0\eta_0\dot{\gamma}^2(\lambda_0/\lambda_\infty)}{1 + k_2\varepsilon_0\varepsilon\beta^2\phi E^2},$$

$$c = \lambda^{-1} - \frac{k_0\eta_0\dot{\gamma}^2}{1 + k_2\varepsilon_0\varepsilon\beta^2\phi E^2} + k_1\left(\frac{\lambda_0}{\lambda_{\mathrm{E}}}\right)\varepsilon_0\varepsilon\beta^2\phi E^2$$

Let us consider the case of vanishing shear rate (i.e., $b \ll 1$). Here, the initial viscosity of the suspension is close to the zero shear rate viscosity, and, furthermore,

$$c = \lambda^{-1} + k_1\left(\frac{\lambda_0}{\lambda_{\mathrm{E}}}\right)\varepsilon_0\varepsilon\beta^2\phi E^2$$

Under these conditions Eqs. (16) and (17) can be solved for the viscosity to give:

$$\eta = \frac{\eta_0}{(c/a) + \mathrm{e}^{-at}} \tag{18}$$

For weak electric fields and low shear rates, the viscosity grows slowly as a function of time with rate proportional to E^2. Under strong electric fields, the viscosity growth with time is exponential, and at long times the viscosity approaches the limit.

$$\eta = \eta_0\left(\frac{\lambda_{\mathrm{E}}}{\lambda_0}\right) = \eta_{\mathrm{E}} \tag{19}$$

where η_{E} is the limiting viscosity at high electric fields. At short times and in the case where $a \gg c$, Eq. (18) gives the proportionality of the characteristic time for structure formation with the viscosity and electric field, i.e., $t_a \propto \eta/E^2$.

Now, let us consider the limit where the flow is strong ($b \gg 1$). In this case, structure induced by the electric field collapses with a rate that is a function of time, shear rate and electric field. The expression for the viscosity from Eqs. (16) and (17) is:

$$\eta = \frac{\eta_0}{\sqrt{1 + 2bt}} \tag{20}$$

Initially, the reference viscosity is the zero shear-rate viscosity. Asymptotic analysis of Eq. (20) shows that at long times, for weak electric fields, the viscosity decreases with a rate proportional to $(\dot{\gamma}\sqrt{t})^{-1}$, whereas under strong electric fields, the viscosity is proportional to $E/\dot{\gamma}\sqrt{t}$. In the latter case, the ratio of the electric field to the shear rate controls the viscosity decrease with time. It is noteworthy to mention that the rate of fragmentation of the kinetic model (Eq. (3)) is independent of the electric field, which agrees with the limit under weak electric fields of Eq. (20).

For the general case of a viscoelastic fluid, specific particular cases may be derived. For instance, when the electric field is equal to zero, Eqs. (6), (15) and (16) give:

$$A = \frac{\lambda_0}{\lambda'} = \frac{\eta_0}{\eta} \tag{21}$$

$$\frac{\mathrm{d}A}{\mathrm{d}t} = \frac{(1-A)}{\lambda} + k_0\left(\frac{\eta_0}{\eta_\infty} - A\right)\underline{\underline{\tau}} : \underline{\underline{D}} \tag{22}$$

where η_0 and η_∞ are the zero-shear rate and infinite shear rate viscosities. If the fluid is Generalized Newtonian, i.e., $\boldsymbol{\tau} = 2\eta D$, Eqs. (16) and (22) reduce the Fredrickson model for suspensions [6]. It is known that this model accounts for time-dependent phenomena occurring in an inelastic suspension of solid particles in a Newtonian solvent. On the other hand, when the flow field vanishes, and considering steady-state, i.e., $\mathrm{d}A/\mathrm{d}t = 0$, the following expression for the viscosity is obtained:

$$\eta = \frac{\eta_{\mathrm{E}}(1 + k_1\lambda\varepsilon_0\varepsilon\beta^2\phi E^2)}{(\eta_{\mathrm{E}}/\eta_0) + k_1\lambda\varepsilon_0\varepsilon\beta^2\phi E^2} \tag{23}$$

This expression accounts for the variation of the suspension viscosity with the electric field in a quiescent state. For vanishing electric fields, the viscosity is η_0, while for high electric fields,

the zero shear viscosity is η_E. In the intermediate range of E, there is a quadratic dependence of the viscosity on the electric field, which agrees with the kinetic model prediction for the viscosity (Eq. (5)). Furthermore, Eq. (23) agrees with the asymptotic limit at long times given by Eq. (19) under vanishing shear rates.

Eq. (15) also embodies particular cases, depending upon the magnitude of each of its terms. For weak flows or under weak electric fields, the first term in the r.h.s. of Eq. (15) predominates, and hence Maxwellian behavior with characteristic time λ_0 is predicted (i.e., $A \to 1$). Also, this behavior is predicted in those systems where the reformation of the structure occurs very fast (i.e., $\lambda \to 0$). If the flow is the dominant force, then the second term in the r.h.s. is the largest, and hence $A \to \lambda_0/\lambda_\infty$ and the resultant behavior is Maxwellian with characteristic time λ_∞. Finally, if the electric force is the dominant one, then the third term in the right-hand side is the largest, and hence $A \to \lambda_0/\lambda_E$. The dynamics in this case are dominated by the characteristic time λ_E.

In steady simple shear flow, it has been proved [6] that in the absence of electric fields, the apparent yield stress is given by:

$$\tau_{y0} = G_0\sqrt{\frac{\lambda_\infty}{\lambda}} \tag{24}$$

where we have identified k_0 with G_0^{-1}. This identification is justified since the yield stress is assumed proportional to the structure of the material, represented by the elastic modulus.

In the presence of the electric field, Eq. (24) becomes:

$$\tau_y = G_0\sqrt{\frac{(1+k_1\lambda\varepsilon_0\varepsilon\beta^2\phi E^2)(1+k_2\varepsilon_0\varepsilon\beta^2\phi E^2)}{\lambda/\lambda_\infty}} \tag{25}$$

Clearly, for vanishing electric fields, Eq. (25) tends to Eq. (24). On the other hand, as E increases, the apparent yield stress as function of applied electric field approaches the following scaling:

$$\tau_y = \tau_{y0}\sqrt{k_1k_2\lambda}\varepsilon_0\varepsilon\beta^2\phi E^2 \tag{26}$$

The proportionality of the yield stress with the volume fraction of particles and the electric field given by Eq. (26) has been verified experimentally in electrorheological suspensions [22,7,8]. In fact, the so-called "polarization model", attributed the attractive force between particles to Maxwell–Wagner interfacial polarization. Within this framework, the yield stress follows the scaling suggested in Eq. (26). This polarization model shows excellent agreement with data for small particle concentrations and electric fields.

3.1. Conductivity contributions to the electrorheological effect

The increase of the conductivity of the liquid or particles affects the electrorheological response of the suspension. Likewise, conductivity effects become important at high electric fields, modifying the polarization state of the particles. In fact, it is known that conductivity of the suspensions affects negatively the actual polarization of particles, inhibiting the formation of the structures responsible of the electrorheological effect. The non-linear effects of suspension conductivity can be introduced in the model through a term $(1 - k_3\sigma E)$ in the expressions of the kinetic constants, Eqs. (12) and (13), to account for the decrease in polarization due to non-linear conductivity. Eqs. (12) and (13) become:

$$k_0' = \frac{k_0}{1 + k_2(1 - k_3\sigma E)\varepsilon_0\varepsilon\beta^2\phi E^2} \tag{27}$$

$$k_1' = k_1(1 - k_3\sigma E)\phi \tag{28}$$

k_3 is a constant and the suspension conductivity is given in terms of the conductivity of the particle and fluid as follows:

$$\sigma = \phi\sigma_p + (1 - \phi)\sigma_f \tag{29}$$

Upon substitution of Eqs. (27) and (28) into the kinetic Eq. (8), the resulting set of equations accounts for the non-linear conductivity contribution to the electrorheological effect. The immediate consequence of this contribution is the possibility to predict a maximum in the variation of viscosity with electric field, and a decrease in the power-law index of the scaling of the yield stress with electric field, as shown in the experiments [9].

4. Results

The steady-state flow curve must include time-independent data as the shear rate is increased. To determine the region along which the viscosity is independent of time, Fig. 1A and B show the normalized stress-growth coefficient plotted as a function of time in the silicon oil suspension for several electric fields and for two shear rates: 0.1 s^{-1} (Fig. 1A) and 1 s^{-1} (Fig. 1B). Data show that the time required to obtain a truly steady-state exceeds 1000 s and becomes longer as the shear rate is decreased. These experiments reveal that under the electric fields considered, the suspension takes a long time to achieve a steady-state at small shear rates.

Steady-state data for various concentrations of the silicon oil suspension and under several electric fields are depicted in Fig. 2A–D. Model predictions are drawn as dashed and continuous lines. In Fig. 2B and C, the flow curve in absence of electric field is also plotted. Notice that at these concentrations (0.08 and 0.12) the suspension in the absence of electric field is slightly shear-thinning and cannot be considered as Newtonian. Nevertheless, upon application of the electric field, the zero-shear rate viscosity increases three decades. Common to all data, the shear viscosity tends to level off for vanishing shear rates. The increase in the viscosity is observed as the electric field increases, and in it becomes asymptotic at sufficiently high electric fields. This is in qualitative agreement with predictions of Eq. (23). For very high shear-rates, the effect of the electric field decreases as the viscosity approaches the second Newtonian region. The slope of the viscosity versus shear rate in the intermediate shear-rate range approaches −2/3 for low electric fields, but becomes −1 at high fields. This is in remarkable agreement with experimental data [3,10] and also

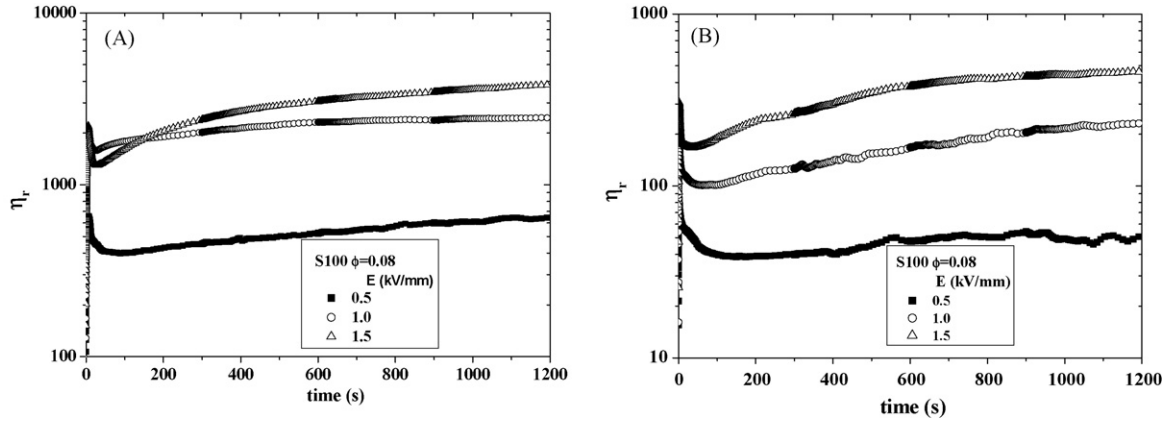

Fig. 1. Normalized stress growth coefficient versus time ($\phi = 0.08$) for three electric fields. (A) Shear rate = 0.1 s^{-1} and (B) shear rate = 1 s^{-1}.

it shows same dependence of the viscosity on shear rate at high electric fields expressed in Eq. (5) of the kinetic model Eq. (3). The model describes the simple shear-thinning behavior of a Bingham plastic fluid at high fields, and at low fields a behavior consistent with the so-called equilibrium droplet model.

In Fig. 3, data and predictions of the relative viscosity (i.e., that normalized with respect to the high shear-rate asymptote) versus Mason number of the silicon oil suspension are shown for electric fields from 0.5 kV/mm to 2 kV/mm, and for particle concentrations from 0.03 to 16 wt%. For Mason numbers higher than unity, the viscosity approaches the second Newtonian plateau, where the flow strength dominates. The model predicts a single function where curves overlap, containing the zero shear-rate Newtonian region for Mason numbers smaller than 10^{-3} and the second Newtonian plateau at high Mason numbers. The slope at intermediate *Mn* is near unity. Agreement between predictions and experimental data is depicted.

In suspensions that exhibit yield stress, the shear viscosity has a slope of −1 as the shear rate diminishes. The fact that

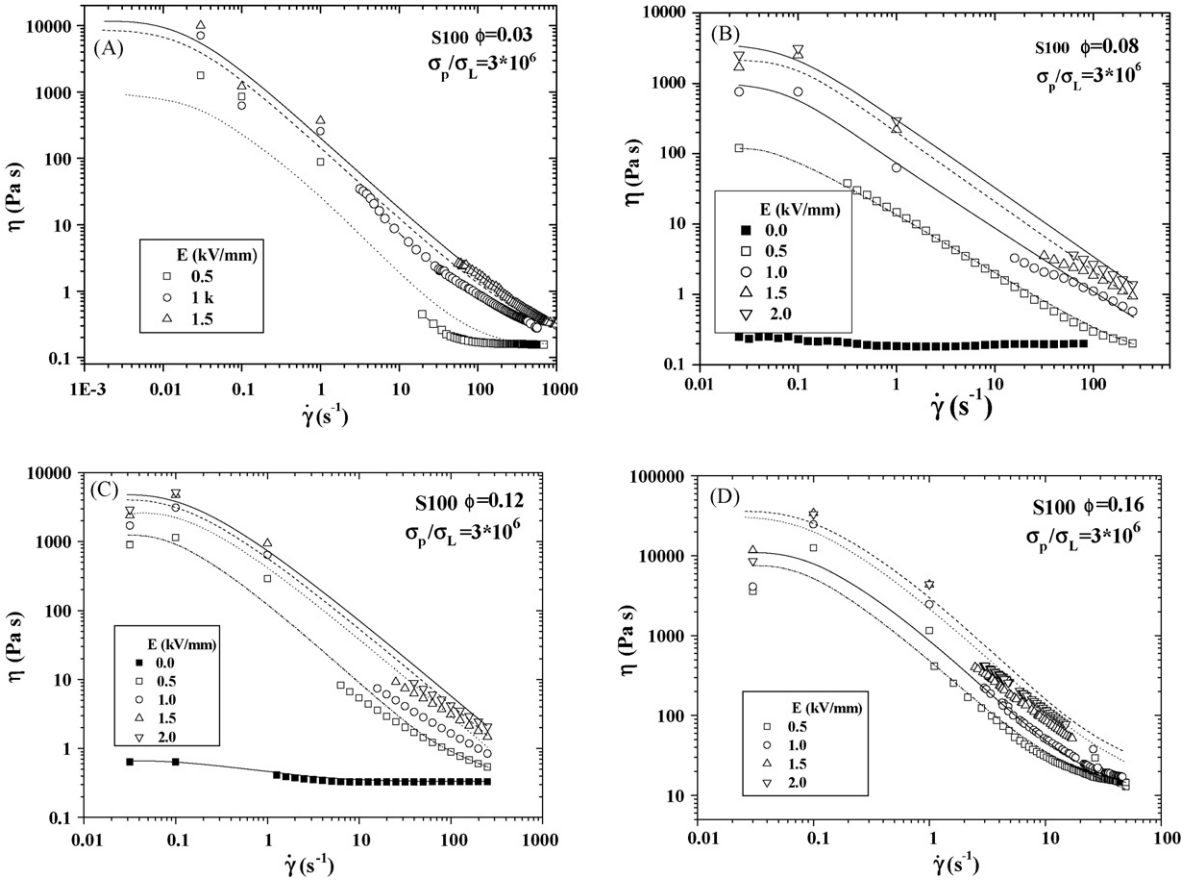

Fig. 2. Data and predictions of the shear viscosity vs. shear rate for various electric fields. $\phi = 0.03$ (A), 0.08 (B), 0.12 (C) and 0.16 (D).

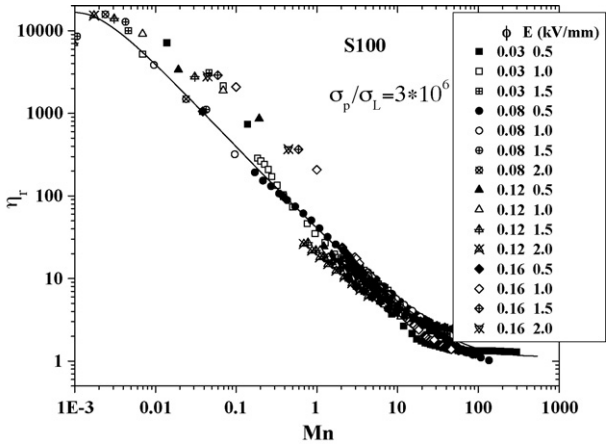

Fig. 3. Predictions and experimental data of the relative viscosity vs. Mason number in the silicon oil suspension, for various electric fields and particle concentrations.

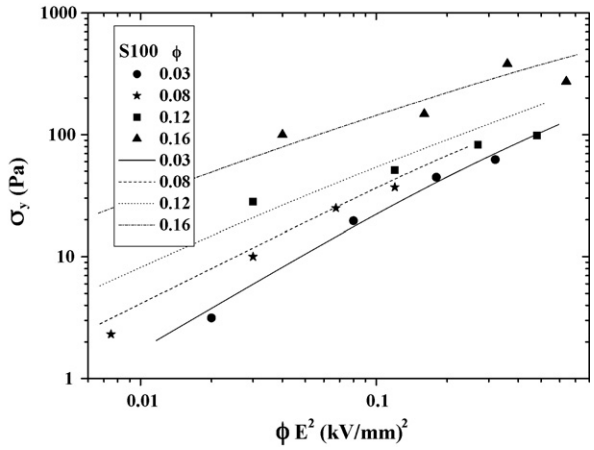

Fig. 5. Plot of the yield stress vs. ϕE^2 of the silicon oil suspension for various particle concentrations. Lines: predictions; experimental data: symbols.

these suspensions attain a Newtonian region, albeit quite narrow at very small shear rates, the yield stress cannot be considered as "real", but only an "apparent yield stress". The yield stress reported here has been determined by extrapolation of the flow curve to zero shear rate. The trend to a Bingham behavior is observable at high electric fields.

Fig. 4 shows a comparison between model predictions and experimental data of the zero shear-rate viscosity versus ϕE^2 in the silicon oil system for the four particle concentrations. Predictions show the trend of the monotonic increase in the viscosity with ϕE^2. The increase in the viscosity follows the scaling suggested by Eq. (23), i.e., a quadratic dependence on E, and a linear dependence with concentration. The asymptotic limit of Eq. (23) at high electric fields renders the value of η_E. As the electric field increases further, experimental data show a trend to level-off of the viscosity, especially at high particle concentrations. The asymptotic behavior of the viscosity with electric field is a manifestation of non-linear conductivity effects, which become substantial as the electric field increases or at high particle concentrations.

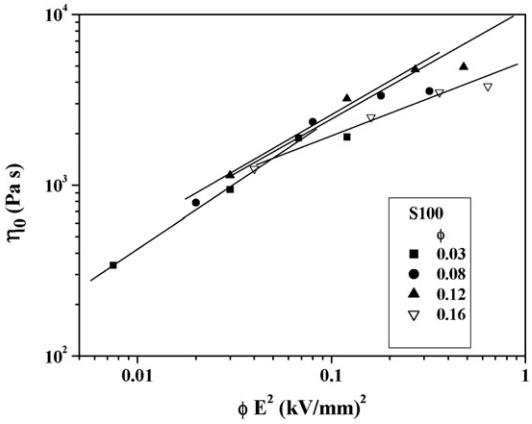

Fig. 4. Predictions (continuous lines) and experimental data (silica particles in silicon oil, symbols) of the zero shear-rate viscosity versus ϕE^2 for four particle concentrations.

Fig. 5 shows predictions and experimental results in the silicon oil system of the yield stress versus the product ϕE^2, for particle concentrations from 0.03 to 0.16. The yield stress increases with particle concentration and electric field squared, and predictions follow closely the scaling given in Eq. (26) at low values of ϕE^2. For high values of the electric field and particle concentration, the scaling approaches $\eta_0 \propto \sqrt{\phi E^2}$. Notice that the slopes of the predicted curves have a value close to one at low electric fields and approach 1/2 at high electric fields.

The following analysis considers an increase in the conductivity of the suspension and its effect upon the electrorheological response of the system. Besides silicon oil, two liquids are examined: dioctyl phthalate (DOP) and tricresyl phosphate (TCP). Conductivity effects are also important as the particle concentration increases or at high electric fields. To account for the decrease in the particle polarization due to conductivity effects, Eqs. (27) and (28) have been proposed. Introducing these equations into the expressions for the viscosity and yield stress for vanishing shear rates (Eqs. (23) and (25)), the consequence of increasing conductivity is to modify the asymptotic behavior of such equations. In fact, in both equations a cubic contribution of the electric field now accounts for a maximum in the yield stress and zero-shear viscosity.

Fig. 6 show data and predictions of the zero shear-rate viscosity versus ϕE^2 when the particle concentration is 0.03 for the three suspending fluids. Predictions for the silicon oil illustrate quantitative agreement with data, except at high electric fields. Nevertheless, predictions show the right trend toward levelling-off in the viscosity along this region. Those for DOP and TCP show good agreement.

Finally, the predictions of the dependence of the yield stress with electric field for the three suspensions is illustrated in Fig. 7 ($\phi = 0.03$) and Fig. 8 ($\phi = 0.16$). In Fig. 7, for low electric fields the predicted dependence of the yield stress with electric field is quadratic, whereas the slope diminishes for higher fields. The limiting slopes at high electric fields with increasing conductivity of the suspensions change from 2 to 3/2 and to 1, the latter observed in the more conductive system. In the more concen-

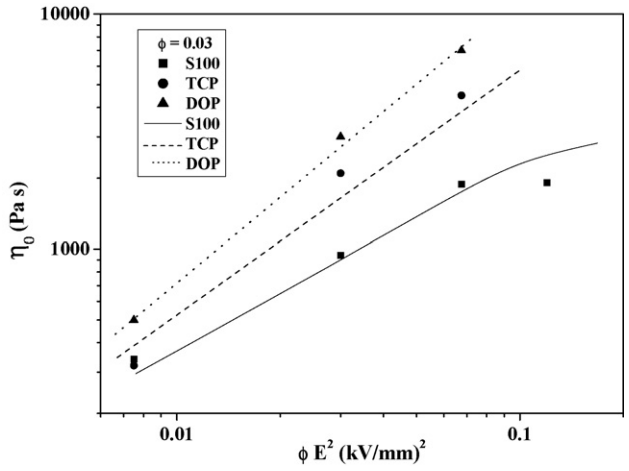

Fig. 6. The zero shear-rate viscosity of the three suspensions with varying conductivity is plotted with ϕE^2, for a particle concentration of 0.03. Model predictions are shown. Experimental data: symbols.

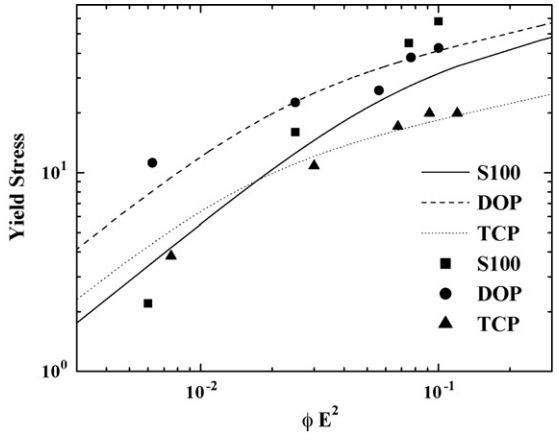

Fig. 7. Predictions and experimental data of the yield stress versus ϕE^2 for three suspensions of varying conductivity. Particle volume fraction is 0.03.

trated suspensions, Fig. 8 depicts model predictions where the limiting slopes at high electric fields can be as low as 0.7 for DOP and TCP, and 1 for the silicon oil. Experimental data shown in Figs. 7 and 8 are in agreement with the trends of the predictions.

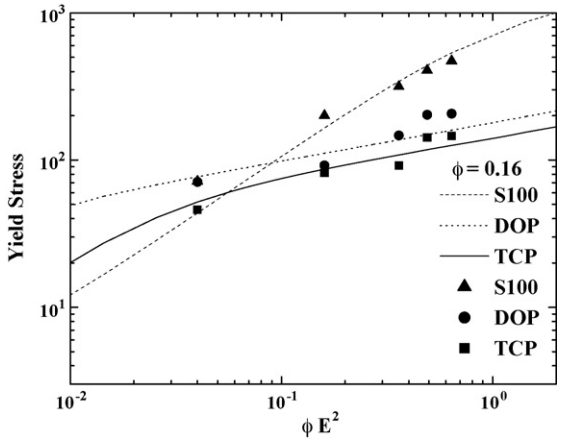

Fig. 8. Predictions and experimental data of the yield stress versus ϕE^2 for three suspensions of varying conductivity. Particle volume fraction is 0.16.

5. Discussion

The model proposed in Eqs. (6)–(8) with the conductivity contributions given in Eqs. (27) and (28) contains eight constants: the time constants λ, λ_0, λ_∞, λ_E and the kinetic constants k_0, k_1, k_2, k_3. The time constant λ_0 is the Maxwell relaxation time and it is related to the zero shear rate viscosity through the relation $\eta_0 = G_0\lambda_0$. λ is related to the structure modification and provides information about the time scale of the reformation process. It appears in the expressions related to the viscosity and yield stress, and controls the onset for shear thinning. When the ratio λ/λ_0 is small (i.e., $\ll$1), the reformation process occurs in a time scale smaller than the time scale of the flow. For large values, the structure does not reform in a time scale of the flow, and time-dependent phenomena (such as thixotropy) may arise. The other two time constants (λ_∞ and λ_E) govern the asymptotic behavior of the suspension at high shear rates (second Newtonian viscosity) and that at high electric fields, respectively.

The kinetic constant k_0 can be identified with the storage modulus G_0 (i.e., with G_0^{-1}), as suggested in Eqs. (24)–(26), and together with k_1, they govern the balance of the flow forces and electric forces. k_1 and k_2 are contained in the expressions for the viscosity (Eq. (23)) and yield stress (Eqs. (25) and (26)), respectively, for vanishing shear rates. Finally, the constant k_3 governs the position of the maximum of the viscosity and yield stress with electric field, and accounts for the non-linear conductivity effects due to high electric fields or high medium conductivity. In summary, each of the phenomenological constants can be evaluated separately from experimental data, and they embody a determined physical meaning.

A relevant prediction of the model is to account for the general features of structure formation kinetics. These are a rapid initial change in particle positions after the application of an electric field to a random suspension, followed by a much slower change at long times. The exponential increase in viscosity followed by a levelling off, represented by Eq. (18), accounts for such behavior, which is described by microscopic models [8,11–14] and verified in experimental studies by See [4] and Klingenberg et al. [12,22,23]. According to Klingenberg et al. [22] at small to moderate particle concentrations, the initial rapid rearrangement is associated with the formation of chains that percolate in the electric field direction and give rise to the remarkable increase in viscosity. The slower coarsening at long times arises from aggregation of these extended structures.

Simulations on the structure formation kinetics [12] predict that the rate of structure changes is proportional to E^2, and that the structure at long time is independent of electric field strength, in agreement with Eq. (18) and with the limit implied in Eq. (19). Furthermore, the time scale of structure formation as predicted by Eq. (18) is proportional to η/E^2, provided that $a \gg c$, which is justified since for an initial random structure (i.e., $\lambda^{-1} \to 0$), and hence $c/a \to \lambda_0/\lambda_E$ and $\lambda_E \gg \lambda_0$. Therefore, the formation of structures is exponential with growth proportional to E^2, and at short times the proportionality of time with η/E^2 arises. At long times Eq. (18) predicts a limiting viscosity given by Eq. (19).

In steady-state flow, Marshall et al. [15] found that the reduced shear viscosity referred to the second Newtonian viscosity plotted with the Mason number (Mn) collapsed to a single function of Mn. The presence of a region where the viscosity varies inversely with Mn for small Mn, suggested the existence of a dynamic yield stress, where electrostatic forces dominate particle dynamics. For large Mn, flow forces dominate and the viscosity becomes independent of the Mason number. Experimental data can be described well by the Bingham model:

$$\frac{\eta}{\eta_\infty} = \frac{\mathrm{Mn}^*}{Mn} + 1 \quad (Mn > 0) \tag{30}$$

where Mn^* is a material constant, equivalent to a dimensionless dynamic yield stress. Predictions of the present model also show a collapse to a single function of Mn, as depicted in Fig. 3. Furthermore, the model predicts a region of slope -1 at low Mn as in a Bingham plastic. The Bingham model predicts a sharp transition at the onset of the second Newtonian region ($Mn = 1 = \mathrm{Mn}^*$), whereas the present model shows a more gradual transition, in agreement with experiments, and with the fact that as the shear rate increases, a more gradual degradation of the structure is feasible instead of an instantaneous degradation predicted by the Bingham model. The non-Bingham behavior is indeed associated with the gradual breakup of field-induced structures [7,8,16] observed experimentally [17].

The model presented here gives a clear indication of the value of the dynamic yield stress, namely, that arising within the region where the apparent shear viscosity should scale inversely proportional to the shear rate. Stokesian dynamics simulations [7,8] predict that at sufficiently low values of Mn, the hydrodynamic contributions of the viscosity become only 10% of the total viscosity and that the electrostatic contributions increase steadily with decreasing Mn. At values of Mn around 2×10^{-4}, where the rheology becomes dominated by electrostatic forces, the hydrodynamic contribution to the viscosity appears to plateau. This is in qualitative agreement with results presented in Fig. 3.

Electrorheological models have focused on the fact that the most drastic field-induced rheological effects are found at small shear rates. In particular, they examine the region where the yield stresses are predominant, and analyze the dependence of the yield stress on the electric field. Yield stress data significantly deviate from the scaling given by Eq. (26) at high electric field strengths [19]. Experimental data [18] reveal that the yield stress is proportional to the square of the electric field at low fields and approaches $E^{3/2}$ at high fields. As the gap between conducting particles in the fluid decreases (increasing particle concentration) the electric response of the fluid becomes non-linear under high electric field strengths. This non-linear conductivity effect was incorporated with the bulk conducting particle model [19] giving rise to a yield stress model which predicts a proportionality between the yield stress and the field with a power-law index of 3/2. This power-law has been verified in several systems [20,21]. The model presented here accounts for the deviation and lowering of the exponent of the electric field. Exponents lower than 3/2 are also predicted.

6. Conclusions

The model proposed here describes in a phenomenological manner many manifestations of the electrorheological behavior of non-Brownian suspensions. In particular, the model predicts the right dependence of the structure formation kinetics with time and electric field, and many of the observed trends in the fragmentation kinetics. It accounts for the variation of the shear viscosity with shear rate and electric field, predicting a single function when data is plotted with the Mason number, in agreement with experiments. It gives the right slope viscosity-shear rate when the electric field is near zero ($-2/3$) and when it approaches high field strengths (-1). Furthermore, the model predicts the increase in viscosity with electric field and saturation at high fields under quiescent conditions and a maximum in the viscosity with electric field due to non-linear conduction. Finally, the model accounts for the dependency of the yield stress with electric field, which is quadratic at low fields, but deviates at high fields (around 3/2), once again, due to non-linear conduction. Analytical expressions were provided for the relevant material functions, from which is possible to estimate the value of the model parameters by performing independent experiments.

Acknowledgements

Financial support from CONACYT project 31123-U and IIE project 11794 are gratefully acknowledged.

Appendix A. Supplementary data

Supplementary data associated with this article can be found, in the online version, at doi:10.1016/j.colsurfa.2007.03.051.

References

[1] L. Rejón, F. Bautista, O. Manero, J. Coll. Surf. A: Physicochem. & Eng. Aspects 301 (2007) 63.
[2] B. Khusid, A. Acrivos, Phys. Rev. E 52 (1995) 1669;
B. Khusid, A. Acrivos, Phys. Rev. E 54 (1996) 5428.
[3] J.E. Martin, J. Odinek, J. Rheol. 39 (1995) 995.
[4] H. See, M. Doi, J. Phys. Soc. Jpn. 60 (1991) 2778.
[5] L. Rejón, I. Castañeda, O. Manero, Coll. Surf. A: Physicochem. & Eng. Aspects 182 (2001) 93.
[6] A.G. Fredrickson, AICHE J. 16 (1970) 436.
[7] R.T. Bonnecaze, J.F. Brady, J. Chem. Phys. 96 (1992) 2183.
[8] R.T. Bonnecaze, J.F. Brady, J. Rheol. 36 (1992) 73.
[9] T. Hao, Adv. Coll. Interf. Sci. 97 (2002) 1.
[10] T.C. Halsey, J.E. Martin, D. Adolf, Phys. Rev. Lett. 68 (1992) 1519.
[11] R. Tao, Q. Jiang, Phys. Rev. Lett. 73 (1994) 205.
[12] D.J. Klingenberg, F. van Zwol, C.F. Zukoski, J. Chem. Phys. 91 (1989) 7888.
[13] N.K. Jaggi, J. Stat. Phys. 64 (1991) 1093.
[14] W.R. Toor, J. Coll. Interf. Sci. 156 (1993) 335.

[15] L. Marshall, C.F. Zukowski, J.W. Goodwin, J. Chem. Soc. Faraday Trans. 85 (1) (1989) 2785.
[16] R. Tao, J.M. Sun, Phys. Rev. Lett. 67 (1991) 398.
[17] T.C. Jordan, M.T. Shaw, IEEE Trans. Elect. Insul. 24 (1989) 849.
[18] C.W. Wu, H. Conrad, Int. J. Mod. Phys. B 13 (1999) 1713.
[19] L.C. Davis, J. Appl. Phys. 81 (1997) 1985.
[20] C.W. Wu, H. Conrad, Phys. Rev. E 56 (1997) 5789.
[21] X. Tang, C.W. Wu, H. Conrad, J. Rheol. 39 (1995) 1059.
[22] M. Parthasarathy, D.J. Klingenberg, Mater. Sci. Eng. Reports 17 (1996) 57.
[23] D.J. Klingenberg, C.F. Zukoski, Langmuir 6 (1990) 15.